CRACK PROPAGATION OF BITUMINOUS MIXTURES REINFORCED BY GEOGRIDS USING DIGITAL IMAGE CORRELATION

Freire, Reuber[1] ; Di Benedetto, Hervé[1] ; Sauzéat, Cédric[1] ; Pouget, Simon[2] ; Lesueur, Didier[3]

[1] *University of Lyon / ENTPE, Laboratory of Tribology and System Dynamics (LTDS) (UMR CNRS 5513) 3 Rue Maurice Audin, 69518 Vaulx-en-Velin, France.*

[2] *EIFFAGE Travaux Publics, Direction R&D, 8 rue du Dauphiné, 69960, Corbas Cedex, France*

[3] *Afitexinov, 56 Route de Ferrossière, 38110 Saint-Didier-de-la-Tour, France.*

reuber.freire@entpe.fr

ABSTRACT:

In the rehabilitation of flexible pavements, the reinforcement by geogrids has substantially increased recently, aiming to extend the service life of pavements. This work aims at evaluating the effect of fiberglass geogrid reinforcement in crack propagation of bituminous mixtures. To conduct the research, five pre-notched beams constituted of two bituminous mixtures layers, with and without geogrid, were tested. Two different fiberglass geogrids, maximum strength resistance of 100 and 50kN/m, and two types of emulsion as tack coat to glue the geogrid on the bituminous mixture layers, were combined for fabrication of three reinforced specimens. Also, two unreinforced specimens were also fabricated. One beam is composed by two bituminous mixtures layers glued by emulsion. The last beam, having the same size, is made of a single bituminous mixture layer. The specimens were subjected to the four-point bending notched fracture (FPBNF) tests, designed at the University of Lyon/ENTPE. A 3D Digital Image Correlation (DIC) device was used to determine the strain evolution around the crack and the crack tip location during the tests. The results showed that the effect of the geogrid is clearly noticeable when the specimen is subjected to high strain and the crack starts to propagate into the beams.

KEYWORDS: Geogrid, Reinforcement, Bituminous mixtures, Crack propagation

1. INTRODUCTION

The rehabilitation and maintenance of bituminous pavements are fundamental to assure an optimal state of utilization and safety for the user. In addition, it is necessary to avoid bigger problems in deteriorated roadways that could lead to the complete loss of serviceability. Recently, the use of geogrids has increased as a technical solution to rehabilitate pavements, extend its service life and reduce maintenance costs [1]. They could be used for both rehabilitation and construction of new bituminous pavements [2, 3]. The reinforcement by geogrid can be effective to reduce the main distresses in flexible pavements worldwide, rutting and cracking. According to some authors, fiberglass geogrids are preferable for presenting high-tension resistance and flexibility at once [4]. It is also thermally and chemically stable at mixing temperatures for bituminous mixtures [5], and easily removable by milling in the case of further pavement maintenances. Many works also indicated that the fiberglass geogrid presents better performance to cracking resistance when compared to the other types of geogrids [6, 7, 8, 9]. Geogrids are also effective on the reinforcement of granular structures [10] and concrete pavements [11].

The geogrids have been proposed for controlling reflective cracking since the 1970s when the American Federal Highway Administration (HMA) instituted a program to reduce reflective cracking in roadways [12]. Reflective cracking occurs when cracks, originally present in the underlying pavemen, propagate towards the surface t. Interlayer reinforcement by geogrids was studied since it is believed to work as a stress-relieving and crack-bridging component and thus, effective to delay reflective cracking [7]. In order to evaluate the cracking resistance and propagation for reinforced bituminous mixtures in the laboratory scale, some authors used three points bending (3Pb) test [9, 13, 14, 15], four points bending (4Pb) test [9, 15, 16, 17, 18] and other different bending tests [19, 20, 21, 22]. Besides, some authors used *in situ* experiments by building experimental roads reinforced by geogrids [4, 9]. Mentioned works indicated a noticeable improvement in the performance of the bituminous mixtures due to the reinforcement, retarding the cracks initiation and propagation. Moreover, in recent works, Digital Image Correlation (DIC) technique was found to be an advantageous tool allowing the identification of different failure mechanisms during the crack propagation in reinforced beams and showing the stress-relieving capacity of geogrid reinforcements [9, 13].

This work aims at evaluating the effect of fiberglass geogrid reinforcement, presence, type and tack coat, in crack propagation of bituminous mixtures. To this end, four-point bending notched fracture (FPBNF) tests designed at the University of Lyon/ENTPE according to [23] were performed in five different specimens. To better analyze the tests, 3D Digital Image Correlation (DIC) device was used to calculate the strain field during the crack propagation as well as its tip.

2. SPECIMENS PREPARATION

The bituminous mixture *Béton Bitumineux Semi-Grenu* (BBSG) 0/10, an AC 10 for surface coarses according to the classification in European standards [24] was used to conduct the experimental campaign. The BBSG 0/10 gradation curve is presented in Figure 1(a). It is composed of mineral aggregates with nature rhyodactic and rhyolitic, mineral filler of limestone and 20% of recycled asphalt pavement (RAP) containing 4.75% of old bituminous binder. These aggregates were mixed with 4.40% of new bituminous binder classified as 35/50 by its penetration. The total bituminous binder content (old + new) in the mixture was 5.53%.

The Geogrids used to reinforce the bituminous mixtures are Notex Glass®, presented in Figure 1(b), fabricated and provided by the French company Afitexinov. This reinforcement is composed by fiberglass yarns and polyester knitted veil, both coated with bituminous emulsion. The grids have a square mesh opening of 25mm in the two directions. Two different geogrids were used in the work with variation in the maximum strength resistance: 50kN (C 50/50) and 100kN (C 100/100).

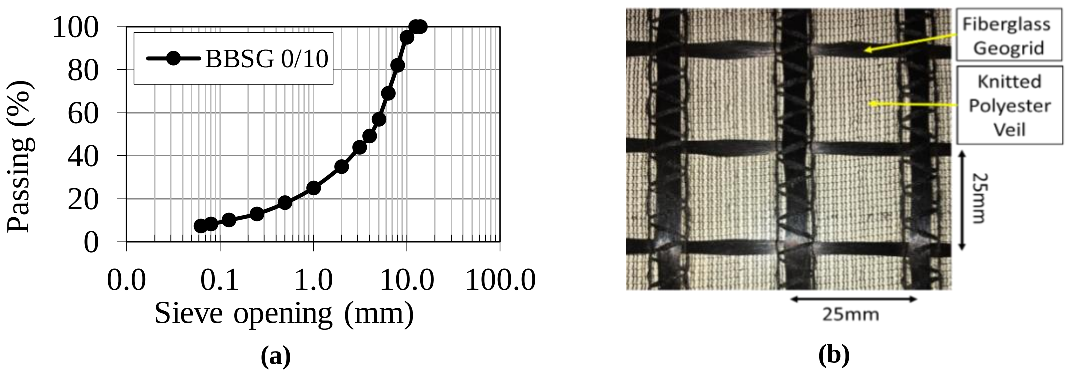

Figure 1. Components of tested specimen: a) Bituminous mixture gradation curve and b) fiberglass geogrid Notex Glass® C 50/50)

Two emulsion of bitumen 160/220 was used as tack coat to glue the geogrid in the middle part of the slabs, one modified by the polymer styrene-butadiene-styrene (SBS) and one without modification. The rate of 800g/m² of residual bituminous binder was used, divided in two applications, one for each geogrid surface.

Five different slabs of 600×400×150mm were fabricated at the French company EIFFAGE Infrastructure using a French wheel compactor [25]. The reinforced slab fabrication is conducted by first compacting half height slab (75mm), after, the first tack coat application is done (400g/m²), followed by the geogrid placement, then the second tack coat application is done (400g/m²) in the geogrid surface and finally the second half height (75mm) slab is compacted. From each slab, a prismatic bar, in a beam shape, with dimensions 550×70×110mm was sawed and a 20mm pre-notch was sawed on its centre-bottom. Finally, to improve DIC accuracy, a speckle pattern is applied on specimen rectangular central area with a thin layer of white acrylic paint and a spray of black paint on it. Figure 2 presents the illustration of the slabs composition and the final beam used for the research development. Five beams were obtained, varying the presence of reinforcement, presence of interface, type of geogrid and type of tack coat. Detailed information, as well as air voids content calculated in the bituminous mixture and tested temperature are presented in Table 1.

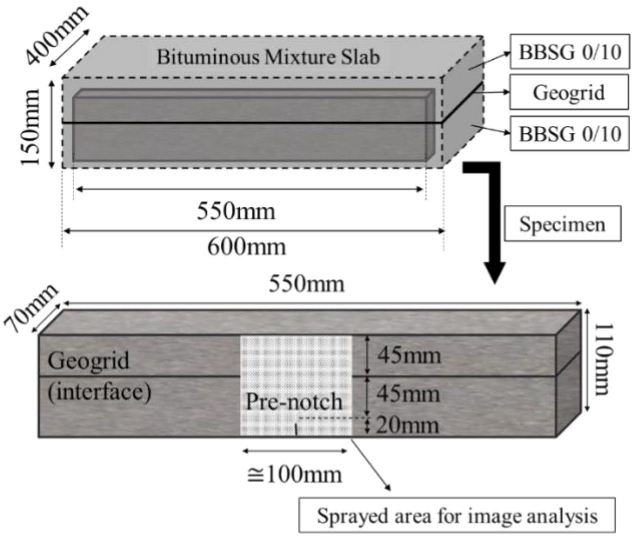

Figure 2. Bituminous mixture slabs obtain with French wheel compactor and beam specimen obtained from sawing

Table 1. Specimen composition, air voids content calculated in the bituminous mixture and tested temperature

Specimen	Geogrid	Tack Coat	Tack Coat content (g/m²)	Air Voids of Bituminous Mixtures (%)	Tested Temperature (°C)
A	No interface	No interface	No Tack Coat	8.0	-1.3
B	Interface without geogrid	160/220 bitumen emulsion	290	5.6	-0.8
C	Notex Glass® C 100/100-25	160/220 bitumen emulsion	2×400	4.8	2.3
D	Notex Glass® C 50/50-25	160/220 bitumen emulsion	2×400	4.3	-2.5
E	Notex Glass® C 100/100-25	SBS Polymer modified bitumen emulsion	2×400	3.9	-2.3

3. EXPERIMENTAL DEVICES AND TEST PROCEDURE

The tests were performed in a servo-hydraulic press INSTRON. This press produces axial loading from its actuator, located in the machine bottom part. The actuator displacement was measured by an integrated transducer and used for controlling the loading performed during the tests. The press was equipped with a load cell with 50kN maximum capacity, which measures the axial stress response during the test. Moreover, three Linear Variable Differential Transducers (LVDT) were placed on supports (LVDT 1 and 3) and on beam centre (LVDT 2) in order to measure the axial displacement in these three points. Beam's deflection was calculated by the LVDT2 measure corrected by the punching effect of the lower supports into the beam, obtained from LVDT 1 and 3 measures. Thus, it was calculated according to Equation (1):

$$Deflection = LVDT2 - \frac{LVDT1 + LVDT3}{2} \quad (1)$$

Figure 3(a) presents a scheme containing all the devices used during the test. Four-point bending notched fracture (FPBNF) test, used for the characterization, was designed at the University of Lyon/ENTPE, more details can be found in previous works developed at the mentioned university [23, 26, 27]. In addition, an adapted thermal chamber coupled with the press [28] is also used for controlling the temperature, measured by a thermal gauge (PT100 temperature probe) fixed on the specimen surface. Furthermore, two cameras were positioned outside the thermal chamber, targeting the sprayed area, in order to perform the DIC method.

The specimens were conditioned at -5°C overnight in a freezer and transferred to the press, where one additional hour of temperature conditioning at the same temperature was done. The FPBNF test was performed at a constant rate of actuator displacement: 0.2mm/min. The test was divided into two steps: first, two cycles of loading/unloading was performed to ensure the contact between specimen and supports. Second, a constant rate of actuator displacement loading was performed until the complete crack propagation throughout the specimen height. Figure 3(b) presents a graphic containing the actuator displacement input and the force (P) response measured during the test for the specimen A.

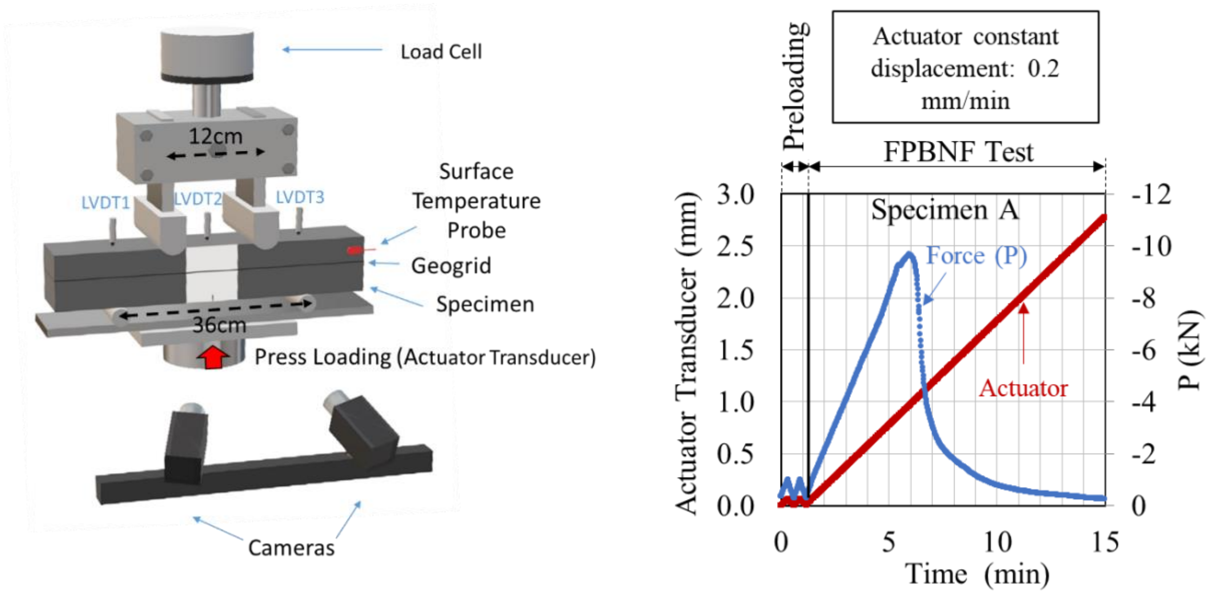

(a) **(b)**

Figure 3. Experimental test device and procedure for FPBNF: a) scheme and measurement device location, b) Actuator displacement and force versus time during the test on specimen A

3.1. Digital Image Correlation

DIC is an optical and contactless measurement technique used to compute the displacement on a specific area of analysis [29]. From simultaneous monochromatic digital images acquired with the aid of two cameras, a 3D image was obtained by image correlation. Each picture is an arrangement of pixels in different shades of grey. The displacement is calculated by comparing subsets of virtual squares containing a small amount of pixel in original and deformed states. More details can be found at [29, 30]. Then, the strain field was also deduced. The software VIC 3D 7 Correlated Solutions, Inc. was employed to perform the images correlation treatment.

Using the software, lines were created every 2mm of specimen height starting from the notch tip. The initial height of the crack tip was the notch size (a_0). Each virtual gauge line was composed of 200 virtual points. For each point, the horizontal strain (ε_{xx}) was calculated composing the strain field for the given area at instant t. The cracking appearance criteria, useful for crack tip identification, was the same used in previous work at the University of Lyon/ENTPE: ε_{xx} = 0.01m/m [28]. From each virtual gauge line, the strain average ($\varepsilon_{xx\text{-}AVG}$) of its points was calculated and plotted in function of the specimens' height. As the crack propagates through the central region in the analysed area of the specimen, a reduction was applied and only the points presented within the central 50mm were considered in the analysis. Figure 4 presented an explanation of the adopted analysis methodology, and GG means geogrid.

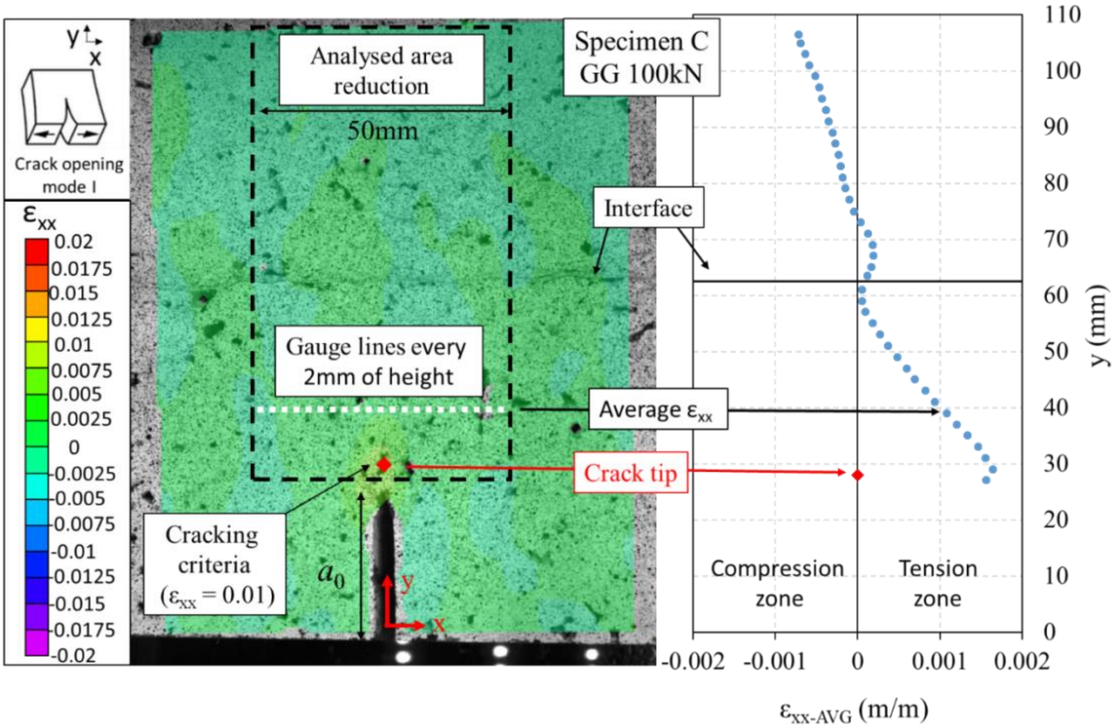

Figure 4. Explanation of analysis performed from data obtained with Digital Image Correlation (DIC) using Vic-3D 7 software

4. CRACK PROPAGATION TEST RESULTS

The curve Force vs Actuator Displacement (from internal press LVDT) was reported for all five tested specimens in Figure 5, where GG means geogrid. Curve peak indicates the cracking initiation and from this point, it starts to propagate. Similar curves in this region confirmed what was observed in [9], the presence of the geogrid does not noticeably influence the load peak value.

For the curves after the peak, it is possible to notice the difference between the reinforced specimens from the unreinforced ones. The fiberglass geogrid improves the cracking propagation resistance of bituminous mixtures. Concerning A (no interface) and B (emulsion interface), very similar behaviour was observed between these unreinforced specimens. Two different plateaus were observed in the reinforced specimens: one for 50kN of maximum resistance geogrid (D) and another one for 100kN of maximum resistance (C and E). The plateau observed for C and E, concerning P, is approximately twice when compared to the one observed for D. Which is coherent with the ratio between the two geogrids maximum resistance. In addition, the curves also indicate, from 1.5mm of actuator displacement, most of the effort is resisted by the geogrids.

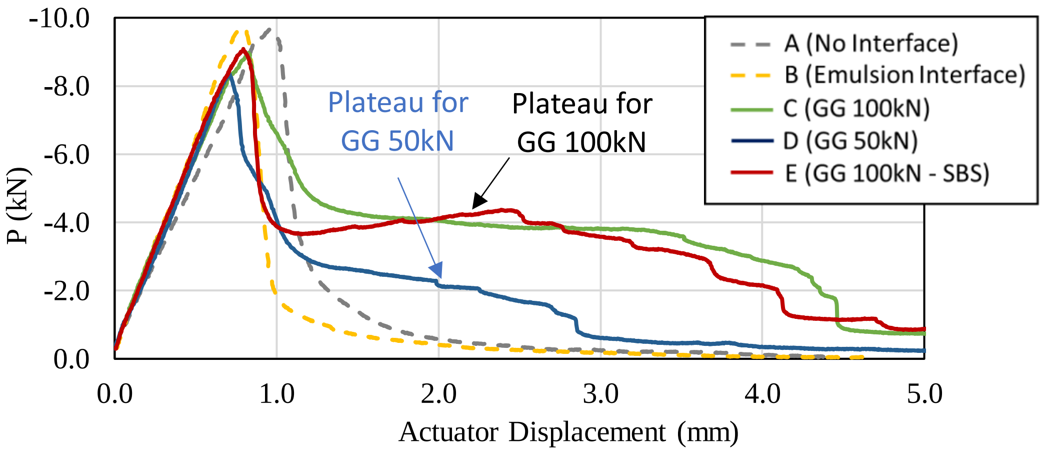

Figure 5. Force vs Actuator Displacement for all tested specimens

The DIC analysis allows the strain field observation during the test. From the method described in section 3.1, it is possible to calculate the average strain in function of beam height during the test at different times *t*. Thus, the positive average strain results from tension stress, while a negative average strain results from compression stress. Figure 6(a) presents the curve P vs Deflection for E and four chosen points of analysis. From Figure 6(b) to (e), the strain field obtained from the software Vic 3D 7 is presented for the four chosen points as well as the curves of average strain in function of beam height. Furthermore, the crack tip is also reported in the figures.

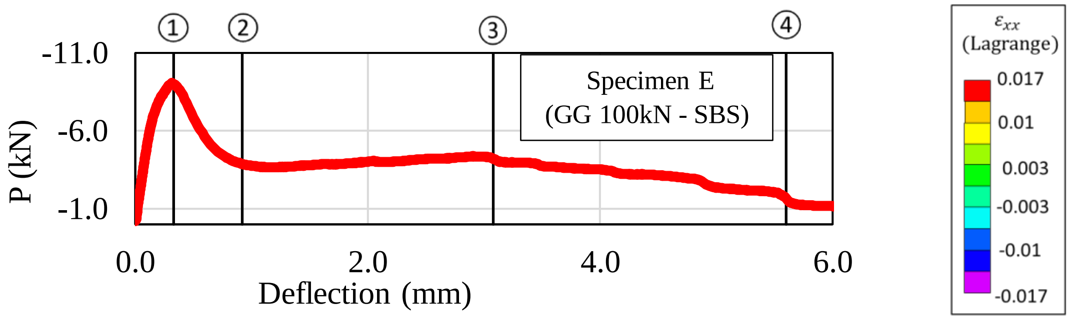

(a) 4 Analysed points indicated on P vs Deflection curve

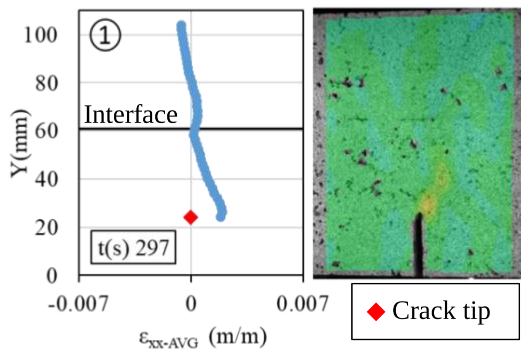

(b) Average ε_{xx} distribution with beam height (t = 297s)

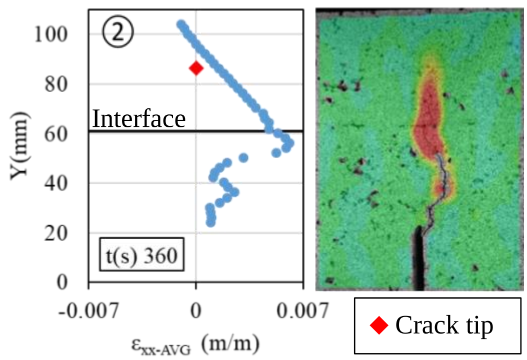

(c) Average ε_{xx} distribution with beam height (t = 360s)

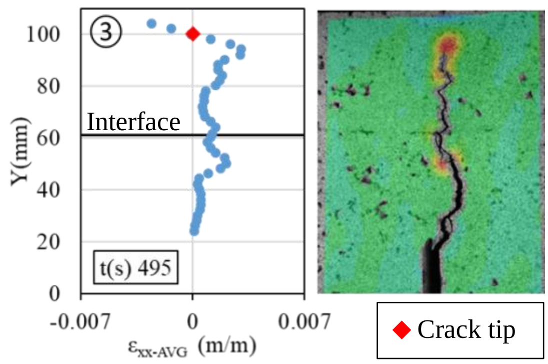

(d) Average ε_{xx} distribution with beam height (t = 495s)

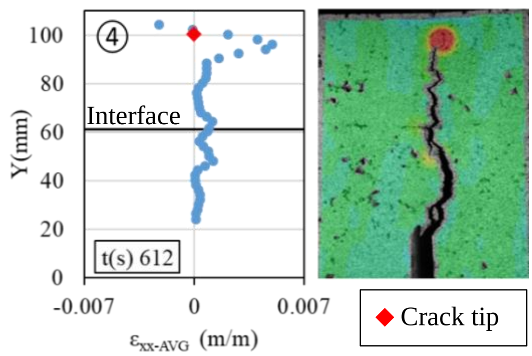

(e) Average ε_{xx} distribution with beam height (t = 612s)

Figure 6. DIC analysis for specimen E (Notex Glass® C 100/100-25, emulsion SBS) at points 1, 2, 3 and 4

First chosen point presents the strain information obtained at the force peak, which represents the crack propagation initiation. From Figure 6(b), it can be observed a non-linearity at the interface level, caused by the geogrid. In Figure 6(c) observing the strain field for the beginning of the plateau, it can be noticed that the crack has already passed through the geogrid in direction to the top of the beam. Thus, the geogrid has effectively started to support loading, reinforcing the bituminous mixtures by a crack-bridging mechanism.

Finally, the same analysis was repeated for all specimens, and the authors decided to choose the peak point of each specimen in order to compare them. Figure 7 presented the curve obtained for A specimen (unreinforced and no interface), which is mostly linear, as expected. Figure 7(a) presents it when compared to B (interface) and D (50kN) and Figure 7(b) when compared to C (100kN) and E (100kN and SBS).

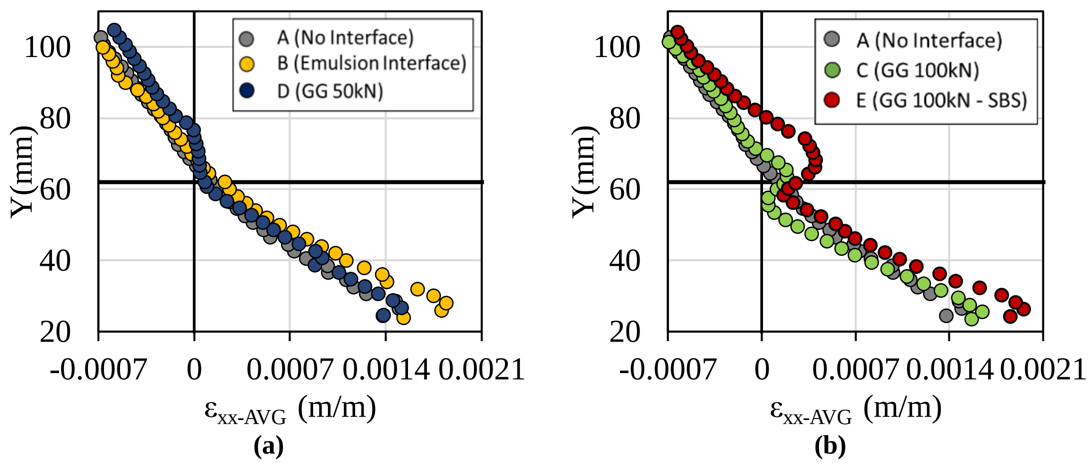

Figure 7. $\varepsilon_{xx\text{-}AVG}$ **at different heights for the five tested specimens at peak load point (point 1 in figure 6)**

From Figure 7, the geogrid interface causes a non-linearity in the curves. However, this is not observed for the B specimen, which contains interface glued by emulsion only. Thus, for B specimens, the interface does not significantly affect the crack propagation. For interfaces containing geogrid, its thickness could be four or five times thicker than the interface without geogrid. In addition, the amount of emulsion presented in the interface to glue the geogrid is 2.8 times bigger than the interface simple. Therefore, the non-linearity observed is caused by geogrid influence, interface thickness, and emulsion quantity and quality. Concerning the SBS emulsion modification, its effect can be seen when compared to the same specimen with non-modified emulsion. The way this non-linearity relates to the so-called stress-relief mechanisms must be further clarified.

5. CONCLUSION

The presented work presented a DIC analysis during FPBNF tests in reinforced and unreinforced specimens. The major conclusions are listed as follows:

- The presence of an interface, containing or not a geogrid, does not influence the peak load, which is an indication of crack propagation initiation
- Geogrids increase drastically the resistance of the beam to crack propagation. A plateau zone is observed were load is mainly balanced by geogrid strength (crack-bridging)
- DIC technic is useful and efficient for calculating the strain field and the crack tip during the test
- The non-linearity observed in $\varepsilon_{xx\text{-}AVG}$ in function of height during the test is caused by geogrid influence, interface thickness, and emulsion quantity and quality

ACKNOWLEDGEMENTS

The authors express their sincere gratitude to the Brazilian public organization CNPq (*Conselho Nacional de Desenvolvimento Científico e Tecnológico*) for providing the PhD grant of first author, and the French companies EIFFAGE Infrastructures and Afitexinov for the technical support and material providing.

REFERENCES

[1] de Bondt A.H., “20 years of research on asphalt reinforcement. Achivements and future needs.” Proceeding of the 7th International RILEM Conference on Cracking in Pavements, Delft. 2012.

[2] Geosynthetic Material Association. Handbook of Geosynthetics, USA, 2002.

[3] Cost Action 348. Reinforcement of pavements with steel meshes and Geosynthetics (REIPAS). Final report of a European Concerted Research Action Designated as COST Action 348, 2006.

[4] Nguyen, M.L., Blanca, J., Kerzrého, J.P. and Hornych, P. (2013). "Review of glass fibre grid use for pavement reinforcement and APT experiments at IFSTTAR." Road Mater Pavement. 14 (1), 2014, 287-308. DOI: 10.1080/14680629.2013.774763

[5] Darling J.R. and Woolstencroft J.H. “Fibreglass pavement reinforcements used in dissimilar climatic zones for retarding reflective cracking in asphalt overlays.” Proceedings of the 5th International RILEM Conference on Cracking in Pavements, 435 - 442, 2004.
[6] Lytton R.L., “Reinforcing fiberglass grids for asphalt overlays.”, Texas Transportation Institute Report for Bay Mills Limited, Texas A&M University, College Station, Texas, 1988.
[7] De Bondt, A. H. “Anti-reflective cracking design of reinforced asphaltic overlays”, PhD thesis, Delft University of Technology, Netherland, 1999.
[8] Brown S.F., Thom N.H. and Sanders P.J., “A study of grid reinforced asphalt to combat reflective cracking.” Journal of the Association of Asphalt Paving Technologies, Vol.70, 2001, 543-571.
[9] Canestrari, F., Belogi, L., Ferrotti, G. and Graziani, A. “Shear and flexural characterization of grid-reinforced asphalt pavements and relation with field distress evolution.” Materials and Structures, 48(4), 2013, 959–975, DOI : 10.1617/s11527-013-0207-1
[10] Mamatha K.H., Dinesh S.V. and Dattatreya J.K. “Evaluation of flexural behaviour of geosynthetic-reinforced unbound granular material beams”, Road Materials and Pavement Design, 20:4, 2019, 859-876, DOI: 10.1080/14680629.2017.1422790
[11] Al-Hedad A. S. A. and Hadi M. N. S. “Effect of geogrid reinforcement on the flexural behaviour of concrete pavements”, Road Materials and Pavement Design, 20:5, 2019, 1005-1025, DOI: 10.1080/14680629.2018.1428217
[12] Carver, C. and Sprague, C.J. “Asphalt Overlay Reinforcement”, Geotechnical Fabric Report Magazine, 2000, 30-33
[13] Romeo, E. Freddi, F. and Montepara, A. “Mechanical behaviour of surface layer fibreglass-reinforced flexible pavements”, International Journal of Pavement Engineering, 15:2, 2014, 95-109, DOI: 10.1080/10298436.2013.828838
[14] Graziani A., Sangiorgi C., Canestrari F. “Fracture Characterization of Grid-Reinforced Asphalt Pavements.” 8th RILEM International Conference on Mechanisms of Cracking and Debonding in Pavements. RILEM Bookseries, vol 13, 2016, 66-67, DOI: 10.1007/978-94-024-0867-6_9
[15] Zofka A., Maliszewski, M. and Maliszewska, D. "Glass and carbon geogrid reinforcement of asphalt mixtures." Road Materials and Pavement Design, vol, 2016, pp. DOI:10.1080/14680629.2016.1266775
[16] A. Virgili, F. Canestrari, A. Grilli, F.A. Santagata, Repeated load test on bituminous systems reinforced by geosynthetics, Geotextiles and Geomembranes, Volume 27, Issue 3, 2009, 187-195, DOI: 10.1016/j.geotexmem.2008.11.004.
[17] Safavizadeh, S.A., Wargo, A., Guddati, M., & Kim, Y.R., "Investigation of reflexive cracking mechanisms in grid-reinforced asphalt specimens using four-point bending notched beam fatigue tests and digital image correlation." Transp Research Record, (2507), 2015, 29-38. DOI: 10.3141/2507-04
[18] Arsenie, I.M., Chazallon, C., Duchez, J.L. and Hornych, P. “Laboratory characterisation of the fatigue behaviour of a glass fibre grid-reinforced asphalt concrete using 4PB tests.” Road Materials and Pavement Design, 18:1, 2017, 168-180, DOI:10.1080/14680629.2016.1163280
[19] Obando-Ante, J. & Palmeira, E.M., “A Laboratory Study on the Performance of Geosynthetic Reinforced Asphalt Overlays.” International Journal of Geosynthetics and Ground Engeneering, 1: 5, 2015, DOI: 10.1007/s40891-014-0007-x
[20] Gonzalez-Torre I., Calzada-Perez M. A., Vega-Zamanillo A., Castro-Fresno D., “Evaluation of reflective cracking in pavements using a new procedure that combine loads with different frequencies.”, Construction and Building Materials, Volume 75, 2015, 368-374, DOI:10.1016/j.conbuildmat.2014.11.030.
[21] Chantachot T., Kongkitkul W., Youwai S., Jongpradist P., “Behaviours of geosynthetic-reinforced asphalt pavements investigated by laboratory physical model tests on a pavement structure.”, Transportation Geotechnics, Volume 8, 2016, 103-118, DOI:10.1016/j.trgeo.2016.03.004.
[22] Nejad F. M., Asadi S., Fallah S., Vadood M., “Statistical-experimental study of geosynthetics performance on reflection cracking phenomenon”, Geotextiles and Geomembranes, Volume 44, Issue 2, 2016, 178-187, DOI:10.1016/j.geotexmem.2015.09.002.
[23] Nguyen, M. L. & Sauzéat, C. & Di Benedetto, H. & Wendling, L. “Investigation of cracking in bituminous mixtures with a 4 points bending test”. Proceedings of the 6th Rilem Int. Conf. On cracking in Pavement, Ed. Al-Qadi, Scarpas, Loizos, Balkema Pub., pp. 284-293, Chicago, June 2008.DOI:10.1201/9780203882191.ch28.
[24] Association Française de Normalisation (AFNOR), “*Spécifications des matériaux Partie 1: Enrobés bitumineux*” (in French), NF EN 13108-1, Paris, 2007.
[25] Association Française de Normalisation (AFNOR), “ *Mélange bitumineux - Méthodes d'essai pour mélange hydrocarboné à chaud - Partie 33 : confection d'éprouvettes au compacteur de plaque*” (in French), NF EN 12697-33+A1, Paris, 2007.

[26] Nguyen M. L., Sauzéat C., Di Benedetto H., Tapsoba N., "Validation of the Time-Temperature superposition principle for crack propagation in bituminous mixtures", Materials & Structures, volume 46, Issue 7, 2013, pp. 1075-87, DOI: 10.1617/s11527-012-9954-7.
[27] Nguyen M. L., Di Benedetto H., Sauzéat C., "Crack propagation characterization of bituminous mixtures using four-point bending notched specimen test", Road Materials and Pavement Design, Vol 17-1, 2016, pp. 70-86, DOI: 10.1080/14680629.2015.1063535.
[28] Pedraza, A., "Propriétés thermomécaniques d'enrobés multi-recyclés" (in French), PhD thesis, University of Lyon/ENTPE, France, 2018.
[29] Sutton, M. A., W. J. Wolters, W. H. Peters, W. F. Ranson, and S. R. McNeill.. "Determination of Displacements Using an Improved Digital Correlation Method." Image and Vision Computing, 1 (3): , 133-139
[30] Attia, T., Di Benedetto, H., Sauzeat, C., Olard, F. and Pouget, S. "Hollow cylinder apparatus to characterize interfaces between pavement layers." 71st RILEM Annual Week & ICACMS, Chennai, India, Vol. 4, 2017, pp. 401-410.